Observation of giant quadrupole plasmon resonance in C_{60} in fast ion collisions

S. Kasthurirangan,[1,2,*] C.-Z. Gao,[3] P. M. Dinh,[4] L. Gulyás,[5] E. Suraud,[4,6] and L. C. Tribedi[1,†]

[1]*Department of Nuclear and Atomic Physics, Tata Institute of Fundamental Research, Colaba, Mumbai 400005, India*
[2]*Department of Physics, Institute of Chemical Technology, Matunga, Mumbai 400019, India*
[3]*Institute of Applied Physics and Computational Mathematics, Beijing 100088, China*
[4]*Laboratoire de Physique Théorique, Université de Toulouse, CNRS, UPS, F-31062 Toulouse Cedex, France*
[5]*Institute of Nuclear Research of the Hungarian Academy of Sciences (ATOMKI), H-4001 Debrecen, Hungary*
[6]*School of Mathematics and Physics, Queen's University Belfast, University Road, Belfast BT7 1NN, Northern Ireland*

(Received 9 November 2021; accepted 5 July 2022; published 26 July 2022)

Strong perturbation caused due to the Coulomb interaction with fast highly charged ions has been used to probe the quadrupole plasmon excitation in C_{60} fullerene. The electron-emission spectrum arising from a free C_{60} molecule reveals a double-peak structure due to the decay of the giant plasmon resonance. Using a state-of-the-art theoretical approach describing the electron dynamics by time-dependent density functional theory, with an explicit ionic background these two peaks are unambiguously identified as arising from the dipole and quadrupole modes of the plasmon. Furthermore, the electron angular distribution clearly shows a double-well-type distribution which is well reproduced by quadrupole and plasmon resonances. The dipole and quadrupole excitations combined with a long-range postcollisional Coulomb interaction shows excellent agreement with the observed anisotropic angular distribution. The present paper serves as an independent confirmation of the presence of a substantial quadrupole plasmon contribution in molecular systems.

DOI: 10.1103/PhysRevA.106.012820

I. INTRODUCTION

The collective behavior in many-body systems is a phenomenon which manifests itself in various disciplines, including nuclear, atomic, molecular, and condensed matter physics. It is a unique problem, which can neither be completely tackled by single-particle models, nor by statistical models. A common physical problem across all these disciplines is to understand the nature of the collective excitation in general. The nuclear giant multipole resonance [1–3], shape resonances in large atoms, such as Xe [4], the giant plasmon excitation in C_{60} [5,6], and the Mie-type plasmon excitations in metallic clusters and solids [7] are analogous to each other since all of these involve collective excitation. Collective behavior in these systems occurs on completely different energies as well as timescales, spanning many orders of magnitude. However, the physical content being of a similar nature, the understanding of one often leads to the understanding of the other [6,8]. A better understanding of the collective behavior in any of these systems can have far-reaching physical implications for the general study of collective phenomena in matter.

The fullerene C_{60} has been of great interest in atomic, molecular, optical, and nanosciences. It serves as a benchmark system for exploring a large variety of molecular many-body systems, such as polycyclic aromatic hydrocarbon (PAH) molecules [9,10] which has implications towards astrochemistry in the interstellar medium, and large ring-shaped biomolecules, such as DNA and RNA base molecules [11] and halouracils in relation to the radiation damage and nanosensitization in hadron therapy. C_{60} fullerene exhibits a collective oscillation of delocalized σ and π valence electrons giving rise to a giant plasmon resonance (GPR) [5,6,12–19].

Earlier, the plasmon resonance in C_{60} has been described in the literature using a simplistic model consisting of a hollow spherical electron cloud of uniform charge density, with inner and outer radii corresponding to the electron cloud of a C_{60} molecule [20–22]. Such a simplistic model indeed provides good results with respect to the major features of the plasmon response. However, in recent years, theoretical advances coupled with growing computational capability have made fully quantum-mechanical descriptions of these phenomena tenable. Among the great variety of theoretical models, the best compromise between the computational expense and detailed description is achieved by density functional theory (DFT) for the electrons, coupled to the carbon ions by pseudopotentials [23,24].

Several previous experimental works on C_{60} plasmons exist, which include photon-, electron-, and ion-impact studies [18,25–31]. Recent efforts have also been made to theoretically investigate the multipole modes of the plasmon excitation [20,32,33]. In the case of photon impact, it is difficult to excite the quadrupole mode in the leading order (which is a dipole term). Quadrupole excitation using photon impact requires extremely high intensities of radiation, and even then, the relative fraction of the quadrupole plasmon to the dipole plasmon would be very small. In the case of high-energy

*Present address: Department of Physics, University of Mumbai, Vidyanagari, Mumbai 400098, India.
†lokesh@tifr.res.in; Ltribedi@gmail.com

electron impact, the Coulomb perturbation strength is too weak to excite the quadrupole mode with sufficient intensity. If enough energy transfer is made to excite the quadrupole mode, it is more likely that this energy will be redistributed in single-particle excitation modes rather than in collective modes [20,34].

Here, we report a combined experimental and theoretical study on the plasmon excitation in C_{60}. We have used an elegant experimental technique of exciting the plasmon mode by the impact of fast highly charged ions, i.e., Si^{q+} with charge state q and velocity v. The highly charged ions can produce a high perturbation strength (q/v) and can excite the plasmon at a relatively large impact parameter, i.e., more than the radius of fullerene. Furthermore, direct electron emission is the fastest mode of deexcitation of the collective plasmon excitation although there are more ways of relaxation, for example, by photon emission or by statistical electron emission following thermalization of the excited electron cloud [35,36]. We have measured the double-differential cross section (DDCS, i.e., $d^2\sigma/d\epsilon d\Omega$, where ϵ = electron energy, Ω = solid angle) of electron emission from the C_{60} molecule and isolated the contribution due to the plasmon electrons. We compare our results on the plasmon electrons with theoretical calculations using an *ab initio* fully quantum-mechanical description of the electron emission from C_{60} using a time-dependent DFT approach.

II. EXPERIMENTAL AND THEORETICAL DETAILS

A. Experimental details

An Si^{12+} ion beam of energy 3.25 MeV/u was obtained from the tandem Pelletron accelerator at TIFR, Mumbai. The ions were made to collide with a C_{60} vapor target in a high vacuum chamber. The experimental setup was described earlier [10,19,37]. Briefly, the energy (1–300 eV) and angular (30°–150°) distribution spectra of electrons were obtained using an electron spectrometer equipped with an electrostatic hemispherical analyzer [37]. C_{60} powder (99% purity) was heated in a metallic oven at approximately 550 °C to obtain an effusive molecular jet [10,19]. The C_{60} vapor yield was monitored *in situ* using a quartz crystal-based thickness monitor. The total uncertainty in the DDCS was about 20%–25% arising mainly from the vapor-pressure fluctuation, normalization procedure, peak fitting, and counting statistics.

B. Theoretical approach

The formalism used in the present work to predict the electron-emission spectrum is the real-time time-dependent density functional theory (TDDFT) at the level of the time-dependent local density approximation (TDLDA), coupled to a classical description of the projectile ions via pseudopotentials (for details, see Refs. [7,24]). We work with a frozen ionic structure, which is justified in the present study since the timescales of the fast ion Coulomb interaction are so short that the nuclear dynamics may be neglected.

The TDLDA is augmented by a self-interaction correction (SIC) in order to accurately predict the electronic properties, in particular the electron-emission spectrum. A full SIC treatment being computationally cumbersome, the more efficient, but reliable, average-density SIC (ADSIC) is used.

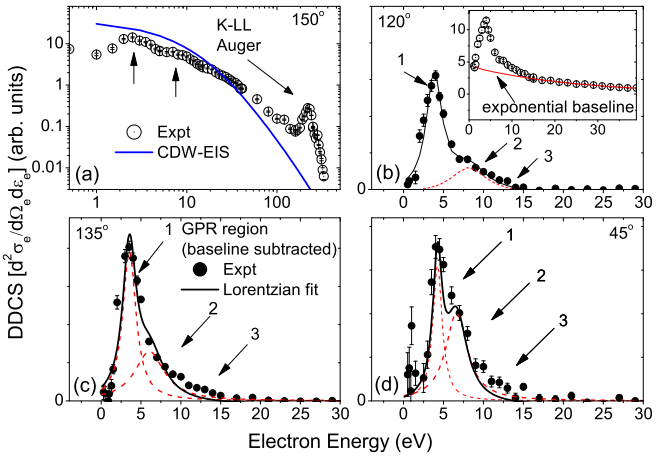

FIG. 1. (a) Electron DDCS at 150°. (b) Inset: DDCS data, with an exponential baseline fit in the GPR region. (b)–(d) Contributions only due to plasmon resonance, obtained after Coulomb-ionization background subtraction. A two-peak structure (labeled as 1,2) is observed, later identified as due to the dipole and quadrupole plasmons

The TDLDA-ADSIC equations are solved numerically on a three-dimensional (3D) grid in coordinate space. The approach is as described in Ref. [35]. The primary observable of interest in the present case is the spectral distribution of dipole and quadrupole strength. In the dipole case, the spectral strength is obtained by excitation of all occupied single-particle wave functions with an instantaneous boost $\varphi_\alpha(t=0) \rightarrow \exp(i\mathbf{p}_{\rm boost}\cdot\mathbf{r})\varphi_\alpha(t=0)$. The strength of $\mathbf{p}_{\rm boost}$ is chosen such that the system remains in the linear regime.

In the quadrupole case, we initially excite all occupied single-particle wave functions with an instantaneous quadrupole $\varphi_\alpha(t=0) \rightarrow \exp(i\lambda\mathbf{Q})\varphi_\alpha(t=0)$, where $\mathbf{Q} = 2z^2 - x^2 - y^2$ and λ is again chosen small enough to remain in the linear domain. The spectral analysis of the dipole or quadrupole response is then attained by Fourier transforming the emerging dipole and quadrupole signals following the approach of Ref. [7].

A comment on temperature effects in the calculations is also in order. Since the C_{60} molecules are produced at a finite temperature (in our case 550 °C, i.e., 820 K), there may be significant temperature effects on the ionic cage. Although it would in principle be possible to incorporate these effects within our TDDFT framework, it is computationally highly expensive to carry out the computation for such a large ensemble. Thus, we have restricted ourselves to the zero-temperature case. As discussed in the results, this is not a serious constraint since the experimental energy resolution smears out the computed spectra quite significantly (see Fig. 2).

III. RESULTS

Figure 1(a) shows the DDCS spectrum of electrons emitted from C_{60} in collisions with Si^{12+} ions, for $\theta = 150°$. The cross section decreases rapidly as a function of electron energy, as is expected for Coulomb ionization [38–40]. Two broad peaks are seen in the low-energy part of the spectrum, which

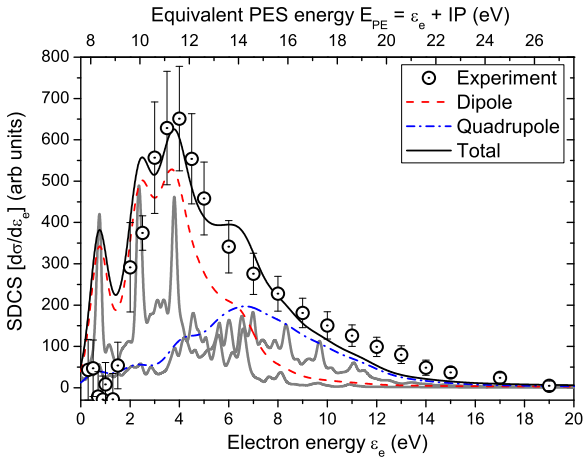

FIG. 2. SDCS of plasmon electrons vs ϵ_e (bottom scale) and $E_{\rm PE}$ (top scale) (see text) along with TDDFT calculations for dipole (red dashed line) and quadrupole (blue dotted line) excitation, both convoluted with detector resolution. Black solid line: total plasmon. Gray lines: original dipole and quadrupole predictions before convolution.

are attributed to the GPR processes. The sharp peak seen at ∼220 eV is from the *K-LL* Auger electron emission. We have also shown the theoretical predictions from the continuum-distorted wave–eikonal initial state (CDW-EIS) model (blue solid line) [41,42]. The theoretical calculation is scaled to match the experimental values at one point (here, 25 eV).

In the inset of Fig. 1(b) the emission in the region below the emission energy of ∼40 eV is fitted with an exponential baseline function in order to isolate the GPR contribution, which is seen as a feature rising above this baseline. This exponential function is seen to fit the electron DDCS from purely atomic targets under identical conditions, and represents the contribution due to the Coulombic interaction between the projectile and the individual electrons. In Figs. 1(b)–1(d), we have shown the data (at three different angles) arising only from the GPR process after Coulomb background subtraction as described above. It is seen that the GPR features can be fitted with two Lorentzian peaks (identified as 1,2). The average energies of these peaks are 3.7 eV ± 0.6 eV and 8.0 eV ± 2.1 eV, respectively. It should be noted that the energy scale is in terms of the ejected electron energy (ϵ_e). In order to compare the observed energies with predictions for the plasmon resonance energy, the ionization potential ∼7.6 eV is to be added (i.e., to get equivalent of photoelectron energy $E_{\rm PE}$) which gives dipole and quadrupole plasmon energies of 11.3 and 15.6 eV, respectively.

The SDCS data ($d\sigma/d\epsilon$) obtained by integrating the DDCS over emission angles are shown in Fig. 2. The electron spectrum is compared with the TDDFT calculations, performed separately for the dipole and quadrupole modes of the plasmon, and indicated by the red (dashed) and blue (dotted-dashed) lines, respectively, with their sum being shown as the black (solid) curve. The theoretical spectra have been convoluted with the detector resolution, which is 6% of the ϵ_e [37]. The original theoretical data are also included (gray lines) to show the extent of the broadening due to detector resolution. We note that the theoretical model is well suited for the prediction of photoionization cross sections [35]. The electrons ejected due to the plasmon excitation have been identified after subtracting the continuum background. As seen in Fig. 2, several major features in the data are reproduced quite well by the theoretical calculation which was originally developed for photoionization.

However, a slight enhancement at around $\epsilon_e = 12$–13 eV ($E_{\rm PE} \sim 20$–21 eV), identified as 3, in the DDCS [Figs. 1(b)–1(d)] (and also seen in the SDCS spectrum in Fig. 2) over the fitted line could not be identified exactly. Whether this could be due to octupole excitation still needs to be confirmed in further work. Projectile ions providing an even higher perturbation strength (q/v) can possibly be suitable to excite octupole excitation. The volume plasmon [17,31] for which $\epsilon_e \sim 30$ eV ($E_{\rm PE} \sim 40$ eV) has not been observed in the present experiment, possibly due to a too small cross section which is comparable to or lower than the Coulomb-ionization background.

Angular distribution of plasmon electrons

The angular distributions of the ejected electrons are mainly governed by the GPR oscillation induced along the beam axis due to the long-range Coulomb field of the fast moving projectile (dwell time $\sim 5 \times 10^{-17}$ s). Therefore the angular distribution is expected to be symmetric about the beam axis (i.e., azimuthal symmetry about the quantization axis). This represents a polarization of the electron cloud, which would lead to angular distributions [$I(\theta)$] of the plasmon electrons. This distribution is symmetric about $\theta = 90^\circ$ and can be expanded in terms of even-order Legendre polynomials $P_n(\cos\theta)$, as follows [43,44],

$$I(\theta) = I_0\{1 + \beta_1 P_2(\cos\theta) + \beta_2 P_4(\cos\theta) + \cdots\}, \quad (1)$$

where θ is the angle of emission of the electron with respect to the beam direction. By analogy with photoelectron emission, the terms in $l = 0, 1, 2, \ldots$ can be interpreted as the contributions of "monopole," "dipole," "quadrupole," etc., configurations of the electron cloud. In the case of C_{60}, these correspond to the respective modes of oscillation of the plasmon.

Figure 3(a) shows the angular distributions of the plasmon electrons for $\epsilon_e \cong 7$ eV. The distribution goes through two local minima, at ∼60°, and ∼120°, indicating the presence of a quadrupole component (the dotted line is a guide to the eye). At this electron energy the contributions from both the dipole and quadrupole terms are expected (see Fig. 2). In typical ion-atom collisions the distributions show a broad peak around 60°–75° which is due to the binary nature of collisions [38–40,45,46]. Such a measurement for methane molecules was carried out *in situ* and not shown here. The asymmetry in angular distribution partly can arise from a postcollisional Coulomb interaction (PCI) between the receding projectiles with the ejected plasmon electrons over a longer timescale, which gives rise to a forward focusing and backward depletion [38,47–49]. The continuum distorted wave–eikonal initial state (CDW-EIS) model [41,42] takes into account the distortion of the electron wave function in the initial and final states due to the influence of two moving Coulomb centers. This provides a reasonable account of the angular asymmetry compared to the one-center model, such as

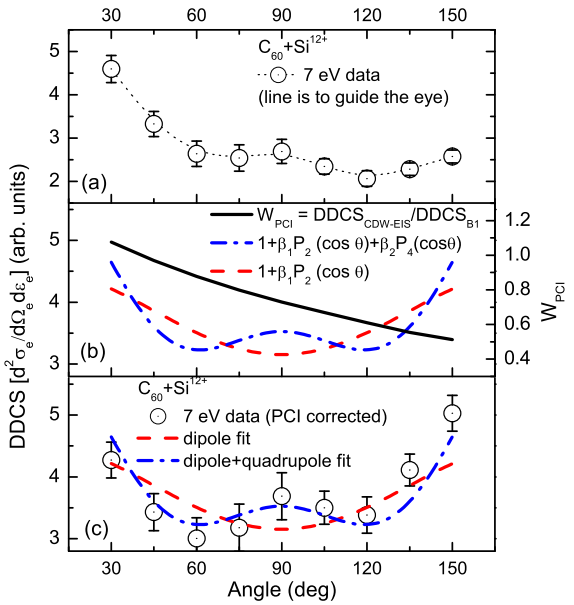

FIG. 3. (a) Angular distribution of electron DDCS at 7 eV. The dotted line is to guide the eye. (b) Predicted distributions: dipole (red dashed line) and dipole+quadrupole (blue dotted-dashed line) mode and $W_{\rm PCI}$ (solid line). (c) Data divided by $W_{\rm PCI}$.

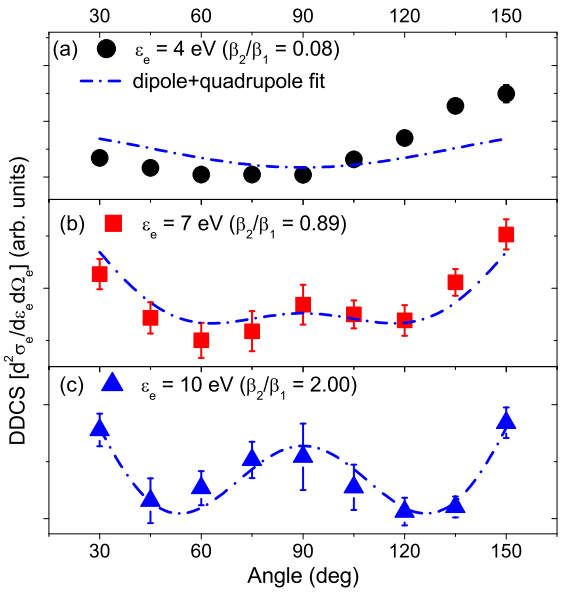

FIG. 4. Angular distribution of electron DDCS of plasmon electrons at 4, 7, and 10 eV, corrected for PCI. The blue dashed-dotted line represents the dipole+quadrupole-type fitting function (see Fig. 3).

first Born (B1) which predicts mostly symmetric distribution about 90°. Thus, the ratio of the CDW-EIS values to that of B1 [i.e., $W_{\rm PCI}(\theta) = ({\rm DDCS})_{\rm CDW\text{-}EIS}/({\rm DDCS})_{\rm B1}$] can yield an approximate correction factor due to the PCI, which is shown as the solid line in Fig. 3(b). We have also shown in this figure the predictions of Eq. (1), truncated to the $l = 1$ dipole term (red dashed line) and the $l = 2$ dipole+quadrupole term (blue dotted-dashed line).

The data in Fig. 3(c) has been corrected by dividing it by $W_{\rm PCI}(\theta)$ and thus can be directly compared with the predictions of Eq. (1). The dipole+quadrupole fit (blue dotted-dashed line) is in excellent agreement with the observed angular distributions for the plasmon electrons. It is obvious that the fitting with the dipole term alone cannot explain the double-minima structure and one needs to include both the quadrupole and the dipole terms, confirming the presence of a quadrupole peak at this energy. A similar earlier measurement with lower charge-state projectiles, such as F^{9+} ions at similar velocity, also revealed a small contribution from the quadrupole term, although it was mostly dominated by the dipole term (see Ref. [19]).

In order to emphasize the relative contributions of the dipole and quadrupole excitations at different electron energies, we extended the analysis at two more electron energies, i.e., 4 and 10 eV (Fig. 4). The data are fitted with a dipole+quadrupole-type fitting function. The relative strength of the dipole and quadrupole contribution can be estimated from the fitting coefficients β_1 and β_2. At 4 eV, the quadrupole to dipole ratio is 0.08, indicating complete dominance of the dipole plasmon. At $\epsilon_e = 7$ eV, the quadrupole to dipole ratio is 0.89, indicating that both modes are contributing significantly. Finally, at $\epsilon_e = 10$ eV, the ratio is 2.03, indicating the dominant role of the quadrupole plasmon over the dipole plasmon.

IV. DISCUSSIONS

We restrict our discussion to two key aspects of this combined experimental and theoretical study of the GPRs in C_{60}. First, we consider the possible physical reason for such a prominent manifestation of the quadrupole mode of the GPR. The excitation of the higher-order multipoles involves larger values of the quantum number l, which can be related to a larger angular momentum transfer. For a fixed value of linear momentum transfer Δp in a particular direction of emission, the angular momentum transfer would be proportional to the impact parameter b (since $\Delta L \sim \Delta pb$) [34]. In order to excite the quadrupole mode of the plasmon oscillation for large b, the Coulomb perturbation has to be of a relatively high magnitude. This condition is met much more readily in the case of collisions with fast heavy ions with a high charge state q. In particular, the dipole plasmon resonance was observed in an earlier experiment involving F^{9+} with $v = 12.7$ a.u. [19]. Here, we have used Si^{12+} ions with $v = 11.4$ a.u. Thus, a comparison of the Coulomb perturbation strength $S = q/v$ in the two cases gives $S_{\rm F} = 0.79$ and $S_{\rm Si} = 1.05$, i.e., a quite significant increase in perturbation strength, which is reflected in the observed excitation of both the dipole and quadrupole modes.

This perturbative regime cannot be readily accessed in keV energy electron collisions due to a high velocity and low charge, thus giving a low perturbation strength. The low charge-state ions may also not be suitable to excite these plasmons. Thus, this paper provides a benchmark for accessing and probing the multipole modes of plasmon oscillations.

The identification of the quadrupole plasmon mode is possible only with equally rigorous and quantum-mechanically complete calculations of the electron spectral distributions. Thus, the present paper also establishes the capability of our TDDFT-based approach to predict the electron spectral

distributions due to the plasmon resonance excited by fast heavy-ion collisions.

In addition, since the C_{60} plasmon deexcites primarily by electron emission [25,26], the angular distributions of the plasmon electrons are of utmost importance since they carry the signature of the multipolarity of the plasmons. The (PCI-corrected) experimental angular distributions and the model predictions are also in very good agreement, leading to an independent understanding of the multipolar nature of the plasmon excitation in C_{60} at high Coulomb perturbation.

V. CONCLUSION

In conclusion, we have demonstrated an approach of using strong perturbation created by fast heavy ions to excite the giant plasmon resonance in C_{60} using fast highly charged ions as a probe, and subsequently demonstrated the signature of plasmon resonance in the electron-emission spectrum. The dipole and quadrupole modes are clearly identified, and compared with state-of-the-art real-time TDDFT calculations which are shown to be in excellent agreement with the observed features. The angular distribution of the electrons, after correcting for the postcollision interaction, clearly reveals the presence of a double-minima structure, thereby serving as an independent confirmation of a substantial quadrupole plasmon contribution in molecular systems.

ACKNOWLEDGMENTS

The authors would like to thank the Pelletron accelerator staff. C.-Z.G. is grateful for the financial support from China Scholarship Council (CSC) (No. [2013]3009). The theoretical part of this work was also granted access to the HPC resources of CalMiP (Calcul en Midi-Pyrénées) under the allocation P1238. Support of the Department of Atomic Energy, Government of India, under Project No. 12P-R&D-TFR-5.02-0300 is acknowledged. L.G. acknowledges the support from the Hungarian Scientific Research Fund (Grant No. K 128621).

[1] K. A. Brueckner and R. Thieberger, Phys. Rev. Lett. **4**, 466 (1960).
[2] F. E. Bertrand, K. van der Borg, A. G. Drentje, M. N. Harakeh, J. van der Plicht, and A. van der Woude, Phys. Rev. Lett. **40**, 635 (1978).
[3] L. A. A. Terremoto, V. P. Likhachev, M. N. Martins, H. J. Emrich, G. Fricke, T. Kröhl, and K. W. Neff, Phys. Rev. C **56**, 2597 (1997).
[4] D. L. Ederer, Phys. Rev. Lett. **13**, 760 (1964).
[5] I. V. Hertel, H. Steger, J. de Vries, B. Weisser, C. Menzel, B. Kamke, and W. Kamke, Phys. Rev. Lett. **68**, 784 (1992).
[6] G. F. Bertsch, A. Bulgac, D. Tománek, and Y. Wang, Phys. Rev. Lett. **67**, 2690 (1991).
[7] F. Calvayrac, P.-G. Reinhard, E. Suraud, and C. Ullrich, Phys. Rep. **337**, 493 (2000).
[8] A. Solov'yov, Acta Phys. Hung. A **14**, 373 (2001).
[9] Y. Ling and C. Lifshitz, Chem. Phys. Lett. **257**, 587 (1996).
[10] S. Biswas and L. C. Tribedi, Phys. Rev. A **92**, 060701(R) (2015).
[11] A. N. Agnihotri, S. Nandi, S. Kasthurirangan, A. Kumar, M. E. Galassi, R. D. Rivarola, C. Champion, and L. C. Tribedi, Phys. Rev. A **87**, 032716 (2013).
[12] J. P. Connerade and A. V. Solov'yov, J. Phys. B: At., Mol. Opt. Phys. **29**, 3529 (1996).
[13] J. P. Connerade, A. G. Lyalin, R. Semaoune, S. K. Semenov, and A. V. Solov'yov, J. Phys. B: At., Mol. Opt. Phys. **34**, 2505 (2001).
[14] L. G. Gerchikov, A. V. Solov'yov, J.-P. Connerade, and W. Greiner, J. Phys. B: At., Mol. Opt. Phys. **30**, 4133 (1997).
[15] J.-P. Connerade and A. V. Solov'yov, Phys. Rev. A **66**, 013207 (2002).
[16] S. W. J. Scully, E. D. Emmons, M. F. Gharaibeh, R. A. Phaneuf, A. L. D. Kilcoyne, A. S. Schlachter, S. Schippers, A. Müller, H. S. Chakraborty, M. E. Madjet, and J. M. Rost, Phys. Rev. Lett. **98**, 179602 (2007).
[17] A. V. Korol and A. V. Solov'yov, Phys. Rev. Lett. **98**, 179601 (2007).
[18] P. Bolognesi, L. Avaldi, A. Ruocco, A. Verkhovtsev, A. Korol, and A. Solov'yov, Eur. Phys. J. D **66**, 254 (2012).
[19] A. H. Kelkar, L. Gulyás, and L. C. Tribedi, Phys. Rev. A **92**, 052708 (2015).
[20] A. Verkhovtsev, A. Korol, and A. Solov'yov, Eur. Phys. J. D **66**, 253 (2012).
[21] D. Östling, P. Apell, and A. Rosén, Europhys. Lett. **21**, 539 (1993).
[22] A. V. Verkhovtsev, A. V. Korol, and A. V. Solov'yov, Phys. Rev. A **88**, 043201 (2013).
[23] C.-Z. Gao, P. Wopperer, P. M. Dinh, E. Suraud, and P.-G. Reinhard, J. Phys. B: At., Mol. Opt. Phys. **48**, 105102 (2015).
[24] C.-Z. Gao, P. M. Dinh, P.-G. Reinhard, E. Suraud, and C. Meier, Phys. Rev. A **95**, 033427 (2017).
[25] S. Cheng, H. G. Berry, R. W. Dunford, H. Esbensen, D. S. Gemmell, E. P. Kanter, T. LeBrun, and W. Bauer, Phys. Rev. A **54**, 3182 (1996).
[26] H. Tsuchida, A. Itoh, Y. Nakai, K. Miyabe, and N. Imanishi, J. Phys. B: At., Mol. Opt. Phys. **31**, 5383 (1998).
[27] U. Kadhane, A. Kelkar, D. Misra, A. Kumar, and L. C. Tribedi, Phys. Rev. A **75**, 041201(R) (2007).
[28] A. H. Kelkar, U. Kadhane, D. Misra, L. Gulyas, and L. C. Tribedi, Phys. Rev. A **82**, 043201 (2010).
[29] J. W. Keller and M. Coplan, Chem. Phys. Lett. **193**, 89 (1992).
[30] J. O. Johansson, G. G. Henderson, F. Remacle, and E. E. B. Campbell, Phys. Rev. Lett. **108**, 173401 (2012).
[31] S. W. J. Scully, E. D. Emmons, M. F. Gharaibeh, R. A. Phaneuf, A. L. D. Kilcoyne, A. S. Schlachter, S. Schippers, A. Müller, H. S. Chakraborty, M. E. Madjet, and J. M. Rost, Phys. Rev. Lett. **94**, 065503 (2005).
[32] M. Schüler, J. Berakdar, and Y. Pavlyukh, Phys. Rev. A **92**, 021403(R) (2015).
[33] M.-X. Wang, S.-G. Chen, H. Liang, and L.-Y. Peng, Chin. Phys. B **29**, 013302 (2020).
[34] L. G. Gerchikov, A. N. Ipatov, A. V. Solov'yov, and W. Greiner, J. Phys. B: At., Mol. Opt. Phys. **31**, 3065 (1998).

[35] P. Wopperer, P. Dinh, P.-G. Reinhard, and E. Suraud, Phys. Rep. **562**, 1 (2015).
[36] E. E. B. Campbell, K. Hansen, K. Hoffmann, G. Korn, M. Tchaplyguine, M. Wittmann, and I. V. Hertel, Phys. Rev. Lett. **84**, 2128 (2000).
[37] D. Misra, K. Thulasiram, W. Fernandes, A. H. Kelkar, U. Kadhane, A. Kumar, Y. Singh, L. GulyÃ¡s, and L. C. Tribedi, Nucl. Instrum. Methods Phys. Res., Sect. B **267**, 157 (2009).
[38] N. Stolterfoht, H. Platten, G. Schiwietz, D. Schneider, L. Gulyás, P. D. Fainstein, and A. Salin, Phys. Rev. A **52**, 3796 (1995).
[39] J. O. P. Pedersen, P. Hvelplund, A. G. Petersen, and P. D. Fainstein, J. Phys. B: At., Mol. Opt. Phys. **24**, 4001 (1991).
[40] D. Misra, A. Kelkar, U. Kadhane, A. Kumar, Y. P. Singh, L. C. Tribedi, and P. D. Fainstein, Phys. Rev. A **75**, 052712 (2007).
[41] P. D. Fainstein, V. H. Ponce, and R. D. Rivarola, J. Phys. B: At., Mol. Opt. Phys. **24**, 3091 (1991).
[42] L. Gulyas, P. D. Fainstein, and A. Salin, J. Phys. B: At., Mol. Opt. Phys. **28**, 245 (1995).
[43] S. Smith and G. Leuchs, in *Advances in Atomic and Molecular Physics*, edited by D. Bates and B. Bederson (Academic, New York, 1988), Vol. 24, pp. 157–221.
[44] B. Cleff and W. Mehlhorn, J. Phys. B: At. Mol. Phys. **7**, 593 (1974).
[45] S. Biswas, J. M. Monti, C. A. Tachino, R. D. Rivarola, and L. C. Tribedi, J. Phys. B: At., Mol. Opt. Phys. **48**, 115206 (2015).
[46] S. Bhattacharjee, S. Biswas, J. M. Monti, R. D. Rivarola, and L. C. Tribedi, Phys. Rev. A **96**, 052707 (2017).
[47] N. V. Maydanyuk, A. Hasan, M. Foster, B. Tooke, E. Nanni, D. H. Madison, and M. Schulz, Phys. Rev. Lett. **94**, 243201 (2005).
[48] R. Moshammer, J. Ullrich, M. Unverzagt, W. Schmidt, P. Jardin, R. E. Olson, R. Mann, R. Dörner, V. Mergel, U. Buck, and H. Schmidt-Böcking, Phys. Rev. Lett. **73**, 3371 (1994).
[49] M. Schulz, R. Moshammer, D. Fischer, H. Kollmus, D. Madison, S. Jones, and J. Ullrich, Nature (London) **422**, 48 (2003).